Experimental versus numerical eigenvalues of a Bunimovich stadium billiard: A comparison

H. Alt,[1,*] C. Dembowski,[1] H.-D. Gräf,[1] R. Hofferbert,[1] H. Rehfeld,[1] A. Richter,[1,2] and C. Schmit[3]

[1]*Institut für Kernphysik, Technische Universität Darmstadt, D-64289 Darmstadt, Germany*
[2]*Wissenschaftskolleg zu Berlin, D-14193 Berlin, Germany*
[3]*Institute de Physique Nucléaire, F-91406 Orsay, France*

We compare the statistical properties of eigenvalue sequences for a $\gamma = 1$ Bunimovich stadium billiard. The eigenvalues have been obtained in two ways: one set results from a measurement of the eigenfrequencies of a superconducting microwave resonator (*real* system), and the other set is calculated numerically (*ideal* system). We show influence of mechanical imperfections of the *real* system in the analysis of the spectral fluctuations and in the length spectra compared to the exact data of the *ideal* system. We also discuss the influence of a family of marginally stable orbits, the bouncing ball orbits, in two microwave stadium billiards with different geometrical dimensions. [S1063-651X(99)12309-2]

PACS number(s): 05.45.Mt, 02.60.Cb, 03.65.Ge, 41.20.Cv

I. INTRODUCTION

Quantum manifestations of classical chaos have received much attention in recent years [1], and for the semiclassical quantization of conservative chaotic systems, two-dimensional billiard systems provide a very effective tool [2,3]. Due to the conserved energy of the ideal particle propagating inside the billiard's boundaries with specular reflections on the walls, the billiards belong to the class of Hamiltonian systems with the lowest degree of freedom in which chaos can occur, and this depends only on the given boundary shape. Such systems are, in particular, adequate to study the behavior of a particle in the corresponding quantum regime, where spectral properties are completely described by the stationary Schrödinger equation. The spectral fluctuation properties of such systems were investigated both analytically and numerically. It has been found that these properties coincide with those of the ensembles of random matrix theory, having the proper symmetry [4,5] if the given system is classically nonintegrable. For time-reversal invariant systems, to which group the billiards investigated here belong, the relevant ensemble is the Gaussian orthogonal ensemble (GOE).

In the last decade this subject was dominated by theory and numerical simulations. About seven years ago experimentalists found effective techniques to simulate quantum billiard problems with the help of macroscopic devices. Due to the equivalence of the stationary Schrödinger equation and the classical Helmholtz equation in two dimensions, one is able to model the billiard by a similarly shaped electromagnetic resonator [6–8].

Theoretical predictions always assume an *ideal* system with a perfect geometry, whereas experiments have been performed with *real* systems. Real microwave cavities—in particular the superconducting ones used here—are usually not machined by the most accurate technique, e.g., milling from a solid block. They are cut from niobium sheet material

which is shaped and afterward electron beam welded. Finally they are chemically etched to clean their inner surface. Their final inner geometry is not accessible to direct measurement, so that their exact geometric properties are not known. In the case of the investigated Bunimovich stadium billiard [9], where $\gamma = a/R = 1$ (see the inset of Fig. 1), the following properties are especially crucial: The radius of curvature of the boundary does not change abruptly but smoothly at the transition from the straight a to the circular section of the boundary [10]. Another point is that the angle at the corners is not exact 90°.

The paper is about the extent to which a comparison of experimental data with theoretical predictions for such billiards is meaningful. Therefore, we want to compare a numerical simulation (calculation of eigenvalues) for a $\gamma = 1$ stadium billiard with a measurement of a real superconducting microwave cavity (measurement of eigenvalues) by studying the statistical properties of the two sequences of eigenvalues.

The paper is organized as follows. In Sec. II the experimental setup and the measurement of the eigenfrequencies
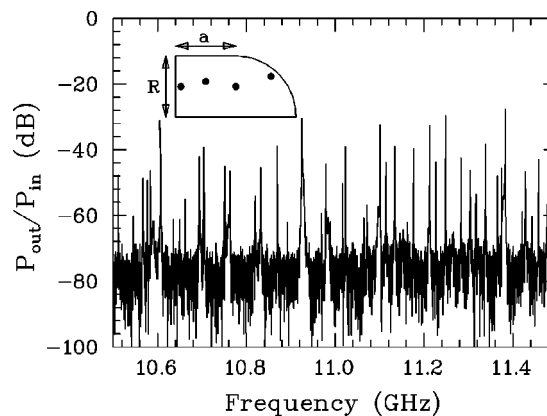

FIG. 1. Typical transmission spectrum of the superconducting $\gamma = 1$ stadium billiard fabricated from niobium in the range between 10.5 and 11.5 GHz taken at 4.2 K. The signal is given as the ratio of output power to input power on a logarithmic scale. The inset illustrates the shape of the resonator and the positions of the antennas.

*Present address: Klöckner Pentaplast, D-56412 Heiligenroth, Germany.

are described, and in Sec. III the numerical calculations are given. A comparison of both sets of eigenvalues is shown in Sec. IV by analyzing their spectral fluctuations.

II. EXPERIMENT

We have experimentally investigated a two-dimensional microwave cavity which simulates a two-dimensional quantum billiard. Here we present results based on measurements using a superconducting niobium cavity, having the shape of a quarter Bunimovich stadium billiard. The billiard has been desymmetrized to avoid superpositions of several independent symmetry classes [11]. Its inner dimensions are $a = R = 20$ cm corresponding to $\gamma = a/R = 1$ (see the inset of Fig. 1), and it has a height of $d = 0.7$ cm, that guarantees a two dimensionality up to a frequency of $f_{max} = c/2d = 21.4$ GHz (c denotes the speed of light).

As in previous investigations [12,13] the measurement of the $\gamma = 1$ stadium billiard has been carried out in a LHe-bath cryostat. This experimental setup is very stable concerning temperature and pressure fluctuations. The cavity has been put into a copper box which was covered by liquid helium, so that a constant temperature of 4.2 K inside the resonator was guaranteed during the whole measurement. The box has also been evacuated to a pressure of 10^{-2} mbar to eliminate effects of the dielectric gas inside the cavity. We were able to excite the cavity in the frequency range of 45 MHz$< f$ < 20 GHz in 10-kHz steps using four capacitively coupling dipole antennas sitting in small holes on the niobium surface; see the inset of Fig. 1. These antennae penetrated only up to a maximum of 0.5 mm into the cavity to avoid perturbations of the electromagnetic field inside the resonator. Using one antenna for the excitation and either another antenna or the same one for the detection of the microwave signal, we are able to measure the transmission as well as the reflection spectra of the resonator using an HP8510B vector network analyzer. In Fig. 1 a typical transmission spectrum of the billiard in the range between 10.5 and 11.5 GHz is shown. The signal is given as the ratio of output power to input power on a logarithmic scale. The measured resonances have quality factors of up to $Q = f/\Delta f \approx 10^7$, and signal-to-noise ratios of up to $S/N \approx 60$ dB, which made it easy to separate the resonances from each other and also to detect weak ones above the background. As a consequence of using superconducting resonators, all important characteristics like eigenfrequencies and widths can be extracted with a very high accuracy [14–16]. A detailed analysis of the raw spectra yielded a total number of 955 resonances up to 20 GHz. To reduce the possibility of missing certain modes with a rather weak electric field vector at the position of the antennae, the measurements were always performed with different combinations of antennae. Thereby the number of missed modes is dramatically reduced below 3–5 in a typical case of a measurement of about 1000 eigenfrequencies. For the $\gamma = 1$ stadium billiard investigated here the 955 detected eigenmodes agree exactly with the expected number calculated from particular geometry of the cavity with the help of Weyl's formula (see Sec. IV below). The measured sequence of frequencies extracted from the experimental spectra forms the basic set of the statistical investigations in Sec. IV.

III. NUMERICAL CALCULATIONS

A. Theory

The problem that we have to solve is to find the eigenvalues of the Dirichlet problem in a billiard, i.e., to solve the following equations:

$$\Delta \Psi(\vec{r}) + k^2 \Psi(\vec{r}) = 0 \quad \text{for } \vec{r} \in \mathcal{D}, \tag{1}$$

$$\Psi(\vec{r}) = 0 \quad \text{for } \vec{r} \in \partial \mathcal{D}. \tag{2}$$

In order to solve these equations, we search for a solution in form of an expansion of regular Bessel functions, so that we write

$$\Psi(\vec{r}) = \Psi(r, \theta) = \sum_{l=-L}^{L} a_l J_l(kr) e^{il\theta}. \tag{3}$$

This expansion is obviously a solution of the first equation, so that we have to solve it under the boundary condition [Eq. (2)]. On the billiard boundary, which may be parametrized by the curvilinear abscissa s, the expansion [Eq. (3)] becomes

$$\Phi(s) = \Psi(r(s), \theta(s)) = \sum_{l=-L}^{L} a_l J_l(kr(s)) e^{il\theta(s)}, \tag{4}$$

which is a periodic function of s. This periodic function may be decomposed in a Fourier series whose coefficients are given by

$$C_n(k) = \frac{1}{2\pi} \int_0^{\mathcal{L}} ds\, \Phi(s) e^{-2in\pi s/\mathcal{L}} = \sum_{l=-L}^{L} a_l C_{n,l}(k), \tag{5}$$

with

$$C_{n,l}(k) = \int_0^{\mathcal{L}} ds\, e^{-2in\pi s/\mathcal{L}} J_l(kr(s)) e^{il\theta(s)}. \tag{6}$$

To satisfy the boundary condition [Eq. (2)], one may impose the equivalent conditions that all Fourier coefficients $C_n(k)$ are zero, at least for $-L \leq n \leq L$, so that we are left with the following linear system in the a_l:

$$\sum_{l=-L}^{L} a_l C_{n,l}(k) = 0, \quad -L \leq n \leq L. \tag{7}$$

For this homogeneous system to have a nontrivial solution, one has the equations

$$D(k) = \det[C_{n,l}(k)] = 0. \tag{8}$$

Thus one is left with the problem of constructing the matrix $C_{n,l}(k)$ and finding the zeros of its determinant $D(k)$. Before going further, we would like to point out the advantages of this method as compared to the well known collocation method. In our method, one may independently vary the number of boundary points used to evaluate the integrals $C_{n,l}(k)$ and the number of partial waves used in the expansion, whereas this is not so in usual boundary methods. (For other methods we refer the reader, e.g., to Refs. [2,17]). Furthermore, it appears clearly that if the billiard is close to a

circle, the matrix is nearly diagonal, so that its determinant is easy to compute numerically, whereas this is not true for plane-wave decompositions. Finally, in contrast with the Green's method, one may always deal with real matrices by decomposing on sine and cosine rather than on exponentials (for time reversal invariant systems). However, one should note that this method does not work for billiards whose boundary consists of several distinct curves (for instance Sinaï billiards).

B. Practical

In practice, the application of the above algorithm depends on the problem one has to solve. For instance, a particular choice of the origin of the coordinates may simplify notably the evaluation of the matrix: For the stadium, a good choice would be the symmetry center of the billiard, so that one may separate easily different symmetry classes. With this choice, the expansion given in Eq. (3), for odd-odd symmetry, become

$$\Psi(\vec{r}) = \Psi(r,\theta) = \sum_{n=1}^{N} a_n J_{2n}(kr)\sin(2n\theta). \qquad (9)$$

Therewith one tabulates the function $D(k)$ in an interval of k such that the number of partial waves needed is constant in the interval

$$k_{\min} \leq k \leq k_{\max}, \qquad (10)$$

with

$$k_{\min} R_{\max} = L \quad \text{and} \quad k_{\max} R_{\max} = L + 2. \qquad (11)$$

In this equation, $R_{\max}$ is the greatest distance of the boundary from the origin, in our case $R_{\max} = R + a$. The number of coefficients a_n may then be taken as

$$N = L/2 + dN, \qquad (12)$$

where dN typically ranges from 0 to 3 or 4. Usually, the positions of the eigenvalues depend very little on this parameter.

The integrals

$$C_{n,m}(k) = \int_0^{\mathcal{L}} ds \, \sin(n\pi s/\mathcal{L}) J_{2m}(kr(s)) \sin(2m\theta(s)) \qquad (13)$$

are evaluated using points regularly spaced along the boundary. As soon as their spacing is such that the fastest varying phase in Eq. (13) changes by less than π in a given step, the evaluation of these integrals is accurate enough to give the position of the zeroes of $D(k)$. In other words, the step Δs used in evaluating Eq. (13) should be such that the condition

$$\frac{N\pi\Delta s}{\mathcal{L}} + \frac{2N\Delta s}{d_{\min}} \leq \pi \qquad (14)$$

is verified, where $d_{\min}$ is the smallest distance of the boundary from the origin, in our case R. With these ingredients, the precise computation of the levels of a rather regular billiards is fast, and does not require powerful computers. Typically,

for the stadium, the computation of the 1000 first levels takes a few hours run on a personal computer, the dimension of the matrices used being smaller than 100. The precision obtained is much better than 1/100th of the average spacing, which is enough for our purpose.

IV. SPECTRAL FLUCTUATIONS

In this section we wish to discuss the statistical properties of the data obtained for the $\gamma = 1$ stadium billiard, as described in Secs. II and III. After a short summary of the general concepts of analyzing spectral fluctuations in Sec. IV A, we present the results for the comparison of the measured and calculated data in Sec. IV B. Finally, in Sec. IV C we compare the influence of a special family of orbits in different Bunimovich stadium billiards.

A. Theoretical background

From the measured (respectively numerically simulated) eigenvalue sequences (''stick spectrum'') the spectral level density $\rho(k) = \Sigma_i \delta(k - k_i)$ is calculated (k is the wave number, and $k = 2\pi/c \cdot f$) and a staircase function $N(k) = \int \rho(k')dk'$ is constructed which fluctuates around a smoothly varying part, defined as the average of $N(k)$. Usually this smooth part $N^{\text{smooth}}(k)$ is related to the volume of the classical energy-allowed phase space. For the two-dimensional billiard at hand with Dirichlet boundary conditions, it is given by the Weyl-formula [18,19]

$$N^{\text{Weyl}}(k) \approx \frac{A}{4\pi}k^2 - \frac{C}{4\pi}k + \text{const.} \qquad (15)$$

where A is the area of the billiard and C its perimeter. The constant term takes curvature and corner contributions into account. Higher order terms [20] are not relevant for the present analysis. The remaining fluctuating part of the staircase function $N^{\text{fluc}}(k) = N(k) - N^{\text{Weyl}}(k)$ oscillates around zero. While Eq. (15) does not contain any information regarding the character of the underlying classical dynamics of the system, the fluctuating part does.

In order to perform a statistical analysis of the given eigenvalue sequence independently from the special size of the billiard, the measured and (respectively calculated) spectrum is first unfolded [21], i.e., the average spacing between adjacent eigenmodes is normalized to 1, using Eq. (15). This proper normalization of the spacings of the eigenmodes then leads to the nearest neighbor spacing distribution $P(s)$, from now on called NND, the probability of a certain spacing s between two adjacent unfolded eigenfrequencies. To avoid effects arising from the bining of the distribution, here we employ the cumulative spacing distribution $I(s) = \int P(s)ds$.

To uncover correlations between nonadjacent resonances, one has to use a statistical test which is sensitive on larger scales. As an example we use the number variance Σ^2 originally introduced by Dyson and Mehta for studies of equivalent fluctuations of nuclear spectra [4,22]. The Σ^2 statistics describes the average variance of a number of levels $n(L)$ in a given interval of length L, measured in terms of the mean level spacing, around the mean for this interval, which is due to the unfolding equal to L:

$$\Sigma^2(L) = \langle (n(L) - \langle n(L) \rangle_L)^2 \rangle_L = \langle n^2(L) \rangle_L - L^2. \quad (16)$$

Furthermore, to characterize the degree of chaoticity in the system, the spectra are analyzed in terms of a statistical description introduced in a model of Berry and Robnik [23] which interpolates between the two limiting cases of pure Poissonain and pure GOE behavior for a classical regular or chaotic system, respectively. The model introduces a mixing parameter q which is directly related to the relative chaotic fraction of the invariant Liouville measure of the underlying classical phase space in which the motion takes place ($q = 0$ stands for a regular system and $q = 1$ for a chaotic system).

The chaotic features of a classical billiard system are characterized by the behavior of the orbits of the propagating pointlike particle. The quantum mechanical analog no longer ''knows'' orbits, but only eigenstates, i.e., wave functions and corresponding eigenenergies. Thus, the individual and collective features of the eigenstates must reflect the behavior of the classical orbits. The semiclassical theory of Gutzwiller [1] assumes that a chaotic system is fully determined through the complete set of its periodic orbits. The influence of the isolated periodic orbits of a billiard is most instructively displayed in the Fourier transformed spectrum of the eigenvalue density $\rho^{\text{fluc}}(k) = dN^{\text{fluc}}(k)/dk$, i.e.,

$$\tilde{\rho}^{\text{fluc}}(x) = \int_{k_{\min}}^{k_{\max}} e^{ikx} [\rho(k) - \rho^{\text{Weyl}}(k)] dk, \quad (17)$$

with $[k_{\min}, k_{\max}]$ being the wave number interval in which the data are taken.

B. Results

In this section we present the results of the analysis of our data using the techniques described in Sec. IV A. We start with a direct one-to-one comparison of both experimentally and numerically obtained data sets, and first perform a comparison with the sequences of the unfolded eigenvalues. To obtain the unfolded eigenvalues, we fit the Weyl formula [Eq. (15)], onto our measured (respectively numerically simulated) spectral staircase $N(k)$. Doing this, one obtains the following parameters of Eq. (15) for the measured data: an area $A_{\text{fit,expt}} = 710.52 \pm 4.12$ cm^2 and a perimeter $C_{\text{fit,expt}} = 113.68 \pm 2.16$ cm; these are very close to the design values $A_{\text{design}} = 714.15$ cm^2 and $C_{\text{design}} = 111.41$ cm. Within the given uncertainties the respective coefficients A and C agree fairly well. From the numerical data which were obtained from a $\gamma = 1$ stadium billiard with area $A = 4\pi$, the coefficient C can be calculated. The fit of the Weyl formula to the numerical data yields values for coefficients A and C within a few per mille of the calculated coefficients. From this we conclude that due to the not well known mechanical imperfections of the billiard, the uncertainties in the average properties of the spectrum expressed through the coefficients A and C of the Weyl formula are larger in the experiment than in the numerical simulations.

With the unfolding indicated above, the different geometrical properties of the *real* and *ideal* billiards are removed and a direct comparison of the first 770 eigenvalues becomes possible. Computing the difference of the experi-
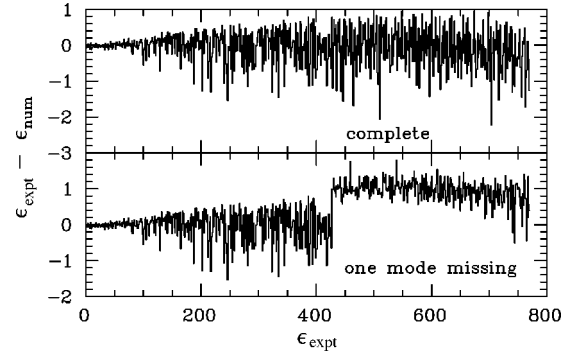

FIG. 2. In the upper part the difference of the unfolded eigenvalues ϵ_{expt}-ϵ_{num} is plotted over the unfolded eigenfrequencies ϵ_{expt} of the experimental data. In the lower part the same curve is shown, but with the 427th mode artificially removed from the experimental spectrum.

mental and the numerical data, ϵ_{expt}-ϵ_{num}, and plotting this difference over the unfolded experimental eigenvalues, the upper part of Fig. 2 is obtained. The curve fluctuates around zero, which is an indication for complete spectra, i.e., no mode is missing. The oscillations appearing in the curve are random, and reflect the fact of how accurate a certain eigenfrequency could be determined experimentally. If only one eigenvalue in the measured sequence is artificially removed, the curve shows a clearly observable step of height 1 at the position where the eigenvalue was dropped. This is demonstrated in the lower part of Fig. 2, where the 427th mode has been removed in the experimental spectrum. More information cannot be extracted from this direct comparison since systematic errors and imperfections have been removed through the unfolding procedure. Therefore, we want to concentrate in the following on the statistical properties of the presented complete sequences of data.

In the next step, we extract the fluctuating part of the staircase function $N^{\text{fluc}}(k) = N(k) - N^{\text{Weyl}}(k)$ from the measured (respectively calculated) eigenvalue sequences (Fig. 3).
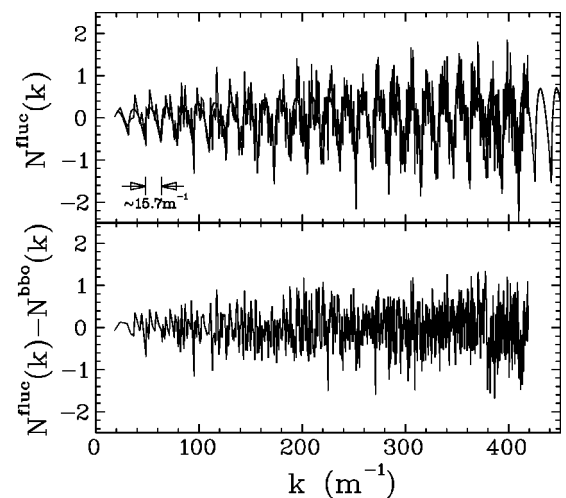

FIG. 3. The histogram in the upper part displays the fluctuating part $N(k) - N^{\text{Weyl}}(k)$ of the staircase function. The full line shows the semiclassical prediction for the bouncing ball orbits (bbo's) according to Eq. (18). The lower part shows $N^{\text{fluc}}(k)$-$N^{\text{bbo}}(k)$, the fluctuating part after subtracting the contribution of the bbo.
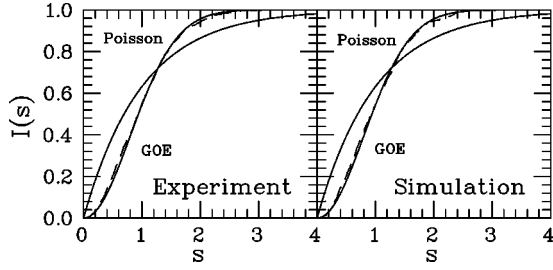
FIG. 4. Cumulative nearest neighbor spacing distribution for the $\gamma=1$ stadium billiards. The dashed curve corresponds to the experimental (left side) and numerical (right side) data, respectively. Also, the two limiting cases (Poisson and GOE) are displayed. The contributions of the bbo are already extracted, so that the data show the predicted GOE behavior.

FIG. 5. Σ^2 statistics of the experimental data set ($\square$) compared with the numerical data ($\triangle$). In the upper part the contribution of the bbo is not extracted; in the lower part it is. The error bars of the data points are a measure of the statistical fluctuations within the given ensemble of eigenvalues in an interval of length L [see Eq. (16)]. Note that the predicted saturation observed in both curves occurs at $L=L_{max}\approx 4$.

As expected, oscillations around zero are seen, also indicating no missing modes.

In the upper part of Fig. 3 a strong enhancement of the amplitude of the fluctuations as a function of wave number k—a characteristic feature of regular systems—is observed, as well as a periodic gross structure with spacing of 15.7 m^{-1} (750 MHz). This behavior of $N^{fluc}(k)$ is caused by the well known family of marginally stable periodic orbits, which bounce between the two straight segments of the billiard, the so-called bouncing ball orbit (bbo's), with length $2r$. The cumulative level density $N(k)$ therefore shows periodic oscillation with a fixed period of $2\pi/2R=15.7$ m^{-1} around the value given by the Weyl formula. These observations can be described [24] by the semiclassical expression for the contribution of the bbo to the spectrum, which reads

$$N^{bbo}(k)=\frac{a}{r}\left(\sum_{1\leq n\leq X}\sqrt{X^2-n^2}-\frac{\pi}{4}X^2+\frac{1}{2}X\right), \quad (18)$$

with $X=(kr)/\pi$. This formula (for a generalization of it in three dimensions, see Ref. [12]) reproduces the mean behavior of the experimental data as shown in the upper part of Fig. 3. After subtraction of this smooth correction, in addition to the expression of Weyl the proper fluctuating part of the level density is obtained, which is plotted in the lower part of Fig. 3. Naturally the same result is obtained for the data from the numerical calculations.

To determine the degree of chaoticity of the investigated $\gamma=1$ stadium billiard, we next calculate the cumulative nearest neighbor spacing distribution $I(s)$ for the fluctuating part of the staircase function corrected by the Weyl and the bbo terms. In Fig. 4 the dashed curve shows the density for a certain spacing s of two adjacent unfolded eigenmodes for the experimental and numerical data. In addition to the data, two limiting cases, the Poisson and GOE distributions, are also displayed. Using the ansatz of Berry and Robnik, one obtains a mixing parameter $q=0.97\pm 0.01$ for the experimental data and $q=0.98\pm 0.02$ for the numerical data. As stated in Ref. [9], the Bunimovich stadium billiard should be fully chaotic, which is expressed through q being very close to unity within the uncertainties of the fitting procedure.

For the Σ^2 statistics, which measure long-range correlations, the effects of the bbo's are strikingly visible; see Fig. 5. Their presence influences the rigidity of the spectrum for large values of length L. A proper handling of these orbits, as
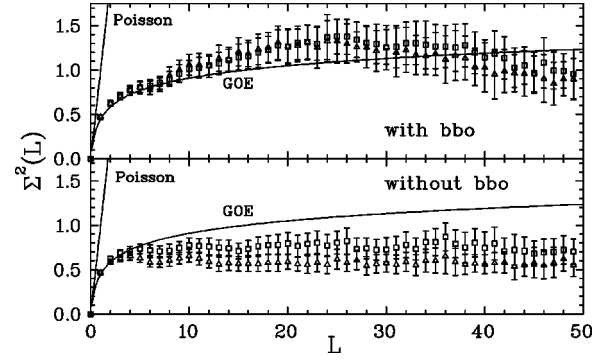
described for the cumulative NND, changes the form of the curve toward the expected GOE-like behavior. In the upper part of Fig. 5 the experimental data ($\square$) and the numerical data ($\triangle$) are displayed for the Σ^2 statistics before removing the contribution of the bbo's. Comparing the Σ^2 statistics of the numerical and experimental data, no significant difference between both data sets can be seen. In contrast to this a small difference between both is extracted when the bbo contribution is removed (lower part of Fig. 5). However, in both cases the Σ^2 statistics very closely follow the GOE prediction up to $L\approx 3.5$, where the distribution saturates. This is in a very good agreement with the theoretical predicted value according to Ref. [25] of $L_{max}\approx 3.8$. This length $L=L_{max}$ also refers to the shortest periodic orbit, which is in the present billiard the bbo. Why is $\Sigma^2(L)$ different for $L>L_{max}$ for the two data sets? This might be due to the fact that the fabricated microwave cavity is a real system with small but existing mechanical imperfections, e.g., a slight nonparallelity of the straight segments of the cavity, which should have its effect on the periodic orbits.

After comparing the statistical measures of the two investigated $\gamma=1$ stadium billiards, we now consider their periodic orbits which are given through the Fourier transformed spectrum of the eigenvalue density $\rho^{fluc}(k)$; see Eq. (17). The lengths of the classical periodic orbits (po's) correspond to the positions and their stability roughly spoken to the height of the peaks in the spectrum. In Fig. 6 the mod-squared of the Fourier transformed of $\rho^{fluc}(k)$ for the experimental (upper part) and numerical (lower part) data are compared. The numerical length spectrum is scaled to the experimental one in such a way that the lowest bbo occurs at the same location in the two Fourier spectra. Then the bbo's, because of their dominating nature in the spectra, were removed [26]. Now a direct comparison between experiment and simulation becomes possible. It can be seen in Fig. 6 that, in addition to the positions of the peaks (lengths of the po's), also their heights (stability of the po's) are almost identical in both spectra.

Let us finally in this subsection return to the bouncing ball orbits. A detailed analysis of these in the experimental billiard, which have lengths $x=nR$ ($n=2,4,6,\dots$) shows that

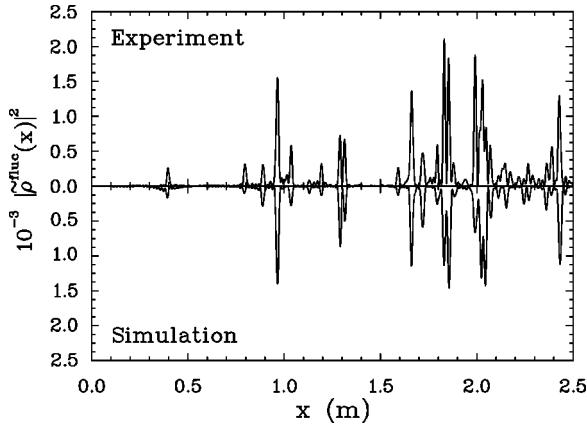FIG. 6. Fourier transform of the fluctuating part of the level density $\rho(k) - \rho^{\mathrm{Weyl}}(k) - \rho^{\mathrm{bbo}}(k)$. The experimental and numerical results are displayed as mirror images. Remnants of the bbo's at $x = 0.4$ m, 0.8 m, and, to a lesser extent at 1.2 m, are still visible.

the distance R between the straight lines of the microwave resonator is not exactly $R = 20$ cm, as specified in the construction, but rather $R = 19.92 \pm 0.05$ cm (the average over the first six recurrences of the bbo's). This means that the two straight segments of the billiard are not exactly parallel. The reasons for this deviation ($\Delta R/R = 4 \times 10^{-3}$) from the design value are, on the one hand, a finite mechanical tolerance during the fabrication ($\approx 3 \times 10^{-3}$) and, on the other hand, effects coming from thermal contractions [27] at low temperatures ($\approx 1 \times 10^{-3}$). This small mechanical imperfection is also the reason for the higher saturation level of the Σ^2 statistics in the experimental data in comparison to the numerical data after removing the bbo contribution (lower part of Fig. 5).

C. Influence of the bouncing ball orbits in different Bunimovich stadiums

In this section we finally discuss the influence of the bouncing ball orbits in the length spectra and in the level statistics of *different* Bunimovich stadium billiards. Therefore, we compare the $\gamma = 1$ stadium discussed so far with an also measured superconducting $\gamma = 1.8$ stadium billiard ($a = 36$ cm and $R = 20$ cm), already presented in Ref. [8]. For this comparison we use the first 1060 eigenfrequencies up to a frequency of 18 GHz.

The interesting features for comparing the two stadiums are the amplitudes of the peaks for the bbo's and not the peaks of the unstable po's, since they naturally have to differ. In Fig. 7 the length spectra of the $\gamma = 1$ and 1.8 stadium billiards are shown. It is clearly visible that the peaks of the bbo's have different heights or amplitudes in the two investigated stadiums. Because the height of the peaks corresponds to the stability of the periodic orbits, these differences can be easily explained. For the $\gamma = 1.8$ stadium the geometrical area on which the bbo's exist is almost twice the area of the $\gamma = 1$ billiard. This correlation between the area of the rectangular part of the billiards with radius R fixed and the amplitude of the peaks for the bbo in the FT was first pointed out in Ref. [28]. This effect is also expressed through the ratio a/R in Eq. (18).
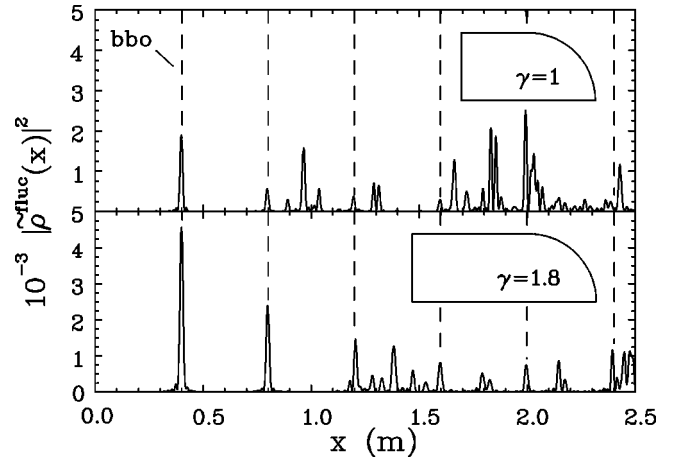

FIG. 7. Experimental length spectra for the $\gamma = 1$ (upper part) and the $\gamma = 1.8$ (lower part) stadium billiards. In both cases the bbo's are not extracted. Obviously the spectra reveal different amplitudes at the positions of the bbo's, which are marked by the dashed lines ($x = nR$, $n = 2,4,6 \ldots$).

The effects of the bbo's are furthermore visible in the statistical measures, as pointed out in Sec. IV B. For the nearest neighbor spacing distribution we have found a Berry-Robnik mixing parameter $q = 0.97 \pm 0.02$ for the experimental $\gamma = 1$ billiard before removing the bbo contribution and $q = 0.98 \pm 0.01$ after removing the bbo contribution. But for the $\gamma = 1.8$ stadium, presented in Ref. [8], the situation differs. There we have a mixing parameter $q = 0.87 \pm 0.03$ for the billiard with bbo's and $q = 0.97 \pm 0.02$ without them. Using the Σ^2 statistics to investigate the long range correlations, the effect of the bbo's for stadiums of different γ values becomes even more obvious. The Σ^2 statistics for the $\gamma = 1.8$ stadium, including bbo's, increase more strongly [see the upper part of Fig. 8 ($\bigcirc$)], than for the $\gamma = 1$ billiard [see the lower part of the same figure ($\square$)]. After removing the bbo contribution one notices that saturation sets in at the same $L_{\max} \approx 4$ for both stadiums. In other words, the shortest po is the same in both stadiums as it should be. The results which have been found are thus in excellent agreement with those predicted in Refs. [28,29], which state that the influence of the bbo's is very small in the $\gamma = 1$ stadium billiard, so that it can be characterized as being the most chaotic stadium.
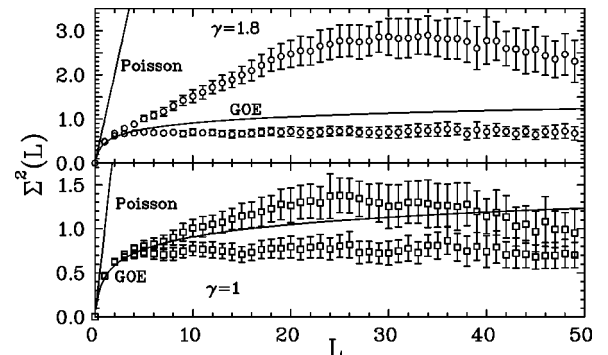

FIG. 8. Comparison of the Σ^2 statistics of the $\gamma = 1.8$ stadium ($\bigcirc$) before (upper curve) and after (lower curve) the extraction of the bbo's contribution, as well as for the $\gamma = 1$ stadium ($\square$).

V. CONCLUSION

In this paper we have shown two different methods, an experimental method and a numerical method, to obtain eigenvalue sequences of a $\gamma = 1$ Bunimovich stadium billiard. A direct comparison of these two data sets clearly reveals that both sets are complete and that no eigenmode is missing. Informations, e.g., accuracy of the measured (respectively simulated) eigenvalues cannot be obtained from this test. Therefore, we analyzed the statistical properties of the billiards. Using the cumulative nearest neighbor spacing distribution $I(s)$, both data sets show the same predicted GOE behavior after removing the contribution of the bouncing ball orbits. The same result is obtained from the Σ^2 statistics, by which we investigated the long range correlations of the eigenvalues. Only the saturation level of the experimental data at large intervals is somewhat above of the level of the numerical data, because the bbo's cannot be removed exactly. The reason for this can be found in the length spectra of the data, which uncovers that the lengths of the bbo's in the experiment deviate slightly from their expected values due to the design of the cavity. The cavity contracts at low temperatures, and its mechanical fabrication is only possible within certain tolerances. On the other hand, we have shown that such small imperfections of the real system do not have any influence on the results of the statistical analysis. Furthermore, we have investigated the influence of the bbo in two different stadium billiards. They clearly have different effects on the respective statistical measures, confirming in particular that the $\gamma = 1$ stadium is even more chaotic than the $\gamma = 1.8$ one.

The comparison of the experimental and numerical eigenvalues was performed to show how accurately the results of the statistical analysis depend on the given method of providing eigenvalues. To obtain information about simple two-dimensional billiards, such as the presented $\gamma = 1$ stadium billiard, numerical calculations sometimes have an advantage, e.g., if one is interested only in eigenvalues. To simulate experiments involving eigenfunctions as in Refs. [13,14] is a different matter. Furthermore, for problems where one is interested in billiards with scatters inside, billiards with fractal boundaries or three-dimensional billiards, etc., the experiment clearly offers a very convenient way to obtain large sets of eigenvalues quickly.

[1] M.C. Gutzwiller, *Chaos in Classical and Quantum Mechanics* (Springer, New York, 1980).

[2] S.W. McDonald and A.N. Kaufman, Phys. Rev. Lett. **42**, 1189 (1979).

[3] M.V. Berry, Proc. R. Soc. London, Ser. A **413**, 183 (1987).

[4] M.L. Mehta, *Random Matrices and the Statistical Theories of Energy Levels*, 2nd ed. (Academic Press, San Diego, 1991).

[5] O. Bohigas, in *Chaos and Quantum Physics*, edited by M.-J. Giannoni, A. Veros, and J. Zinn-Justin (Elsevier, Amsterdam, 1991), p. 89.

[6] S. Sridhar, Phys. Rev. Lett. **67**, 785 (1991).

[7] H.-J. Stöckmann and J. Stein, Phys. Rev. Lett. **64**, 2215 (1990); J. Stein and H.-J. Stöckmann, *ibid.* **68**, 2867 (1992).

[8] H.-D. Gräf, H.L. Harney, H. Lengeler, C.H. Lewenkopf, C. Rangacharyulu, A. Richter, P. Schardt, and H.A. Weidenmüller, Phys. Rev. Lett. **69**, 1296 (1992).

[9] L.A. Bunimovich, Funct. Anal. Appl. **8**, 254 (1974); Commun. Math. Phys. **65**, 295 (1985); Zh. Éksp. Teor. Fiz. **89**, 1452 (1985) [Sov. Phys. JETP **62**, 842 (1985)].

[10] D. Alonso and P. Gaspard, J. Phys. A **27**, 1599 (1994).

[11] E.B. Bogomolny, Physica D **31**, 169 (1988).

[12] H. Alt, C. Dembowski, H.-D. Gräf, T. Guhr, R. Hofferbert, H. Rehfeld, A. Richter, R. Schuhmann, and T. Weiland, Phys. Rev. Lett. **79**, 1026 (1997).

[13] H. Alt, C.I. Barbosa, H.-D. Gräf, T. Guhr, H.L. Harney, R. Hofferbert, H. Rehfeld, and A. Richter, Phys. Rev. Lett. **81**, 4847 (1998).

[14] H. Alt, H.-D. Gräf, H.L. Harney, R. Hofferbert, H. Lengeler,

A. Richter, P. Schardt, and H.A. Weidenmüller, Phys. Rev. Lett. **74**, 62 (1995).

[15] H. Alt, P. v. Brentano, H.-D. Gräf, R.-D. Herzberg, M. Phillip, A. Richter, and P. Schardt, Nucl. Phys. A **560**, 293 (1993).

[16] H. Alt, P. v. Brentano, H.-D. Gräf, R. Hofferbert, M. Phillip, H. Rehfeld, A. Richter, and P. Schardt, Phys. Lett. B **366**, 7 (1996).

[17] M. Sieber and F. Steiner, Phys. Lett. A **148**, 415 (1990).

[18] H. Weyl, J. Reine Angew. Math. Band **141**, 1 (1912); **141**, 163 (1912).

[19] H. Weyl, J. Reine Angew. Math. Band **143**, 177 (1913).

[20] H.P. Baltes and E.R. Hilf, *Spectra of Finite Systems* (Bibliographisches Institut, Mannheim, 1975).

[21] O. Bohigas and M.-J. Giannoni, in *Mathematical and Computional Methods in Nuclear Physics*, edited by J.S. Dehesa, J.M.G. Gomez, and A. Polls, Lecture Notes in Physics Vol. 209 (Springer, Berlin, 1984), p. 1.

[22] F.J. Dyson and M.L. Mehta, J. Math. Phys. **4**, 701 (1963).

[23] M.V. Berry and M. Robnik, J. Phys. A **17**, 2413 (1984).

[24] M. Sieber, U. Smilansky, S.C. Creagh, and R.G. Littlejohn, J. Phys. A **26**, 6217 (1993).

[25] M.V. Berry, Proc. R. Soc. London, Ser. A **400**, 229 (1985).

[26] This, however, was not completely possible—as can be seen from the remnants of the lowest bbo in Fig. 6 at $x = 0.4$ m—due to the numerical uncertainties when Eq. (18) is applied to the data.

[27] H.D. Erfling, Ann. Phys. (N.Y.) **41**, 467 (1942).

[28] A. Shudo and Y. Shimizu, Phys. Rev. A **42**, 6264 (1990).

[29] G. Benettin and J.-M. Strelcyn, Phys. Rev. A **17**, 773 (1978).